

The production of high-energy electrons from the interaction of an intense laser pulse with an underdense plasma

Z. NAJMUDIN, K. KRUSHELNICK, E. L. CLARK,
D. J. COLLING, M. TATARAKIS, A. MODENA, A. E. DANGOR
Plasma Physics, Imperial College of Science and Technology, London,
SW7 2BW, UK; e-mail: z.najmudin@ic.ac.uk

J. FAURE†, V. MALKA‡
Laboratoire Utilisations des Lasers Intenses (LULI), Ecole
Polytechnique, Palaiseau, France

D. GORDON§ and C. JOSHI
University of California, Los Angeles, California 90095, USA

(Received 1 March 2002)

Abstract. The interaction of an intense laser pulse (intensity, greater than $10^{19} \text{ W cm}^{-2}$) has been studied with underdense deuterium plasmas. The laser pulse is found to be self-modulated at the plasma frequency by the Raman forward-scatter instability. Wave breaking of the resulting plasma wave causes high-energy electrons to be accelerated beyond 100 MeV.

1. Introduction

The advent of chirped-pulse amplification has pushed the maximum intensities that can be produced by high-power lasers to ever higher values. Within the next few years, several lasers with powers greater than a petawatt (10^{15} W) will come into operation in research laboratories around the world. It will be possible to focus these lasers to intensities greater than $10^{21} \text{ W cm}^{-2}$. The interaction of such laser pulses with matter is of great interest not only because of the new frontier of physics that can be investigated but also because of the many applications which have been envisaged for such interactions. In particular, these interactions will be the source of high-energy particles with energies of interest to nuclear physics applications.

For example, it has long been supposed that plasma may be an ideal medium for acceleration of particles to extremely high energies [1]. This is due to the extremely high electric fields, which can be supported in plasmas. For a relativistic plasma wave (one with a phase velocity close to the speed of light), the wavenumber is simply $k_p = \omega_p/c$, where ω_p is the plasma frequency:

† Present address: University of California, Berkeley, California, USA.

‡ Present address: Laboratoire Ondes et Acoustique, Ensta, Palaiseau, France.

§ Present address: Plasma Physics Division, Naval Research Laboratory, Washington, DC, USA.

$\omega_p = ne^2/\varepsilon_0 m_e$. The electric field associated with a sinusoidal variation in charge density due to the plasma wave of this density and wavenumber is then simply $E_{\max} = c(m_e/n_0/\varepsilon_0)^{1/2} \approx 0.96[n_0 (\text{cm}^{-3})]^{1/2} \text{V cm}^{-1}$. For $n_0 = 10^{19} \text{cm}^{-3}$, $E_{\max} = 300 \text{GeV m}^{-1}$, about 10^4 times greater than the electric field attainable in present-day high-energy accelerators, owing to the limitations of electrical breakdown. Tajima and Dawson [1], when proposing the use of plasmas for acceleration purposes, suggested several methods of generating such relativistic plasma waves of high amplitude, using either lasers or particle-beam drivers. They also noted that such large amplitude relativistic waves could be produced by instabilities of an intense laser pulse propagating in a plasma.

When an intense laser passes through a plasma, it can be scattered collectively by low-level oscillations within the plasma. Such collective scattering is common in laser–plasma interaction where the laser wavelength can be much greater than the Debye length of the initially cold and dense plasma. Such scattering can be thought of as a scattering off a quanta of plasma oscillations, $\omega_s = \omega_0 \pm \omega_p$, where $\hbar\omega_s$ is the scattered photon energy and $\hbar\omega_0$ is the incident photon energy. The superposition of the incident and scattered photons can result in a modulation of the laser pulse at the plasma frequency ω_p . This modulation through the action of the ponderomotive force can resonantly drive growth of the plasma waves. Since the plasma oscillations have to be in phase with the laser modulations, which travel at the laser group velocity, the plasma wave must have a phase velocity that equals the laser group velocity. For a sufficiently underdense plasma ($n_e \ll n_{\text{cr}} = \varepsilon_0 m_e \omega_p / e^2$), this will be close to the speed of light (since in a plasma the dispersion relation for an electromagnetic wave is $c^2 k^2 = \omega_0^2 (1 - n_e/n_{\text{cr}})^{1/2}$). As the plasma wave grows, so the scattering rate increases, resulting in a distribution of energy to frequency shifted satellites of the initial laser pulse, and a temporal modulation of the laser pulse. Hence in analogy to the scattering from atomic media, this process is called stimulated Raman scattering [2, 3].

The result of this increasing unstable modulation of the laser pulse is an increasing growth in the plasma wave amplitude, so that it is possible for the amplitude of the plasma wave to reach a density perturbation close to the initial ambient density of the plasma wave. When this happens, it becomes possible for the plasma wave to self-trap electrons with sufficient velocity relative to the correlated motion of electrons within the plasma wave. Indeed, if the plasma wave amplitude greatly exceeds the initial ambient plasma density (as it may do, owing to nonlinear steepening of the plasma wave), then a large bunch of electrons that form part of the plasma wave can become dephased (when excessively driven) from the plasma wave and, rather than feeling a returning force, will feel an acceleration from the next phase of the plasma wave. Since in this large-amplitude electric field the electrons can reach relativistic speeds exceedingly rapidly, these electrons can then remain in phase with the accelerating field and can be accelerated to very high energies. This process is known as wave-breaking and can result in the production of an extremely high current of relativistic electrons [4].

2. Laser parameters, target area set-up, spectrometer and electron beam diagnostics

The experiments detailed in this paper were performed at the Rutherford–Appleton Laboratory with the Vulcan: CPA laser. The Vulcan: CPA laser can

generate laser pulses with up to 100 J on target in a 1 ps pulse. Wavefront distortion in the beam due to thermal lensing in the amplifiers is corrected with a static adaptive optic. This allows the beam to be focused to a roughly twice diffraction-limited spot. In the experiments detailed here the laser beam was focused to a spot diameter of approximately $10\ \mu\text{m}$ (full width at half-maximum), resulting in intensities well in excess of $10^{19}\ \text{W cm}^{-2}$, when focused in vacuum.

To prevent ionization defocusing of the laser beam before reaching focus, the laser beam is focused on the edge of a high-density-gradient gas jet. The density profile of the nozzle had been previously measured by interferometry [5]. The nozzle has been optimized to ensure that the vacuum-gas interface is as sharp as possible while retaining a flat density profile within the gas itself. The density of neutrals is varied by changing the backing pressure on the jet and is found to vary almost linearly. Hydrogen or helium is generally used in these experiments, which ensures that the plasma density produced remains uniform, without the intensity-dependent ionization profile that characterizes the interaction with other gases at these laser intensities. This also ensures that the gas jet is free from cluster formation. The gas jet densities measured in this experiment are consistent with the full ionization of the neutrals (2 electrons per molecule) as measured by interferometry [5].

The spectrum of the beam transmitted through the gas jet is attenuated by reflecting off a glass plate, before directing it out of the vacuum chamber. Only reflecting optics are used for transporting the beam, including the lens for collimation and focusing. This ensures a neutral response of the optical system, as well as reducing modifications in the spectrum that may arise from self-phase modulation of the beam passing through optics. Furthermore, the spectral response of the system is calibrated with a black-body emitter placed at the focal plane of the laser beam. The beam is focused on a spectrometer and the spectrum detected with a 16 bit (high-dynamic-range) charge-coupled device camera. The glass plate for collecting the transmitted light has a small hole in it to allow any electrons accelerated by the interaction to pass without scattering or energy absorption. The electron beam is passed into an electron spectrometer, which consists of an evacuated chamber placed between the poles of an electromagnet of radius 5 cm, which has a maximum magnetic field (uniform between the poles) of about 1 T. The dispersed electrons are detected either with individual silicon barrier detectors (of circular area about $1\ \text{cm}^2$ each), or a series of 100 strip detectors $50\ \mu\text{m}$ by 5 cm (total area, 5 cm by 5 cm). In either case, the detectors are biased, and the current generated by ionizing radiation in the depletion region of the diodes is measured on oscilloscopes. When using the strip detectors, two sets of detectors were used simultaneously, one on either side of the undeviated direction of the beam. Thus one set of detectors can be used to detect the accelerated electrons while the other gives a measure of the noise per shot, which principally is from X-rays produced in the collimator, and so are symmetric around the undeviated beam. Indeed the same detectors used to measure noise can be employed to measure ion spectra too since, owing to their slower time of flight in reaching the detectors, they can be easily differentiated from the prompt X-ray noise on the oscilloscope traces. Indeed a combination of time of flight and magnetic deflection can determine the particular ion state detected. However, it is noted that, in these experiments with gaseous targets, one observes no ion signals

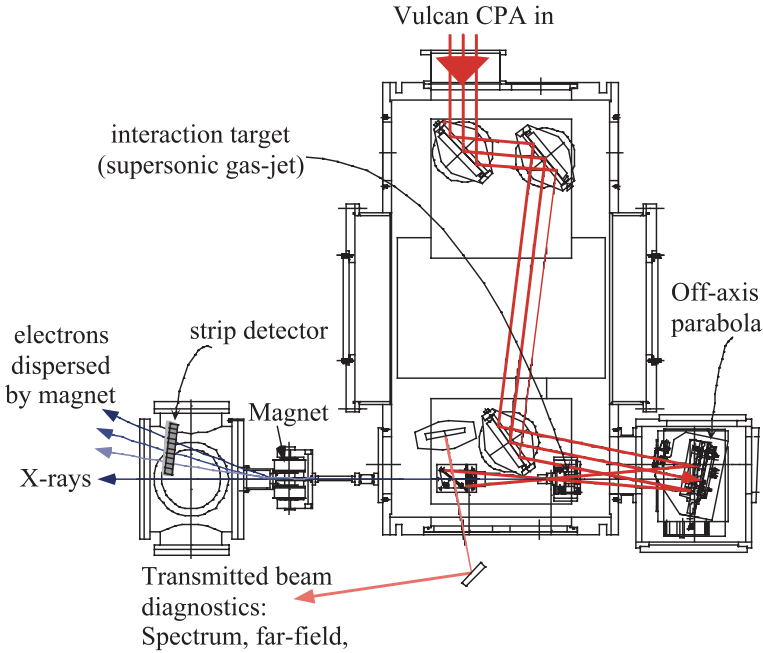


Figure 1. Experimental set-up.

in the directly forward direction. A schematic diagram of the set-up is shown in figure 1.

3. Raman scattering

The laser pulse is found to be highly unstable to plasma Raman-type instabilities. In particular the transmitted beam becomes heavily modulated owing to forward Raman scattering (FRS). Indeed it has been found previously that, as the pulse length decreases from around 3 ps to less than 1 ps, with similar energies, Raman scattering at larger angles is suppressed in favour of direct FRS [6]. However, even at such high intensities, where FRS growth rates are at a maximum [7], it is predicted from the analytic growth rates that the direct FRS cannot grow with sufficient e-foldings to modulate the laser pulse completely, were it to grow directly from thermal noise [8]. Indeed, irrespective of intensity, scattering of laser energy at larger angles (sideways, or preferentially directly backwards) should always have a greater growth rate than direct forward scattering. This is because laser light can be scattered directly by a three-wave process for large-angle scattering, where the incoming photon and the scattered photon can wave match with a plasmon. However, this is not true of FRS, which can only take place through the action of a four-wave process; both upshifted and downshifted scattered waves are required in this mechanism for wavematching. Fortunately three-dimensional particle-in-cell simulations are now possible which can adequately describe the behaviour of the laser beam, including the complex interplay between several different instabilities [9, 10].

It is observed in such simulations that off-angle Raman instabilities do indeed have a much larger growth rate and can cause severe scattering from the front of

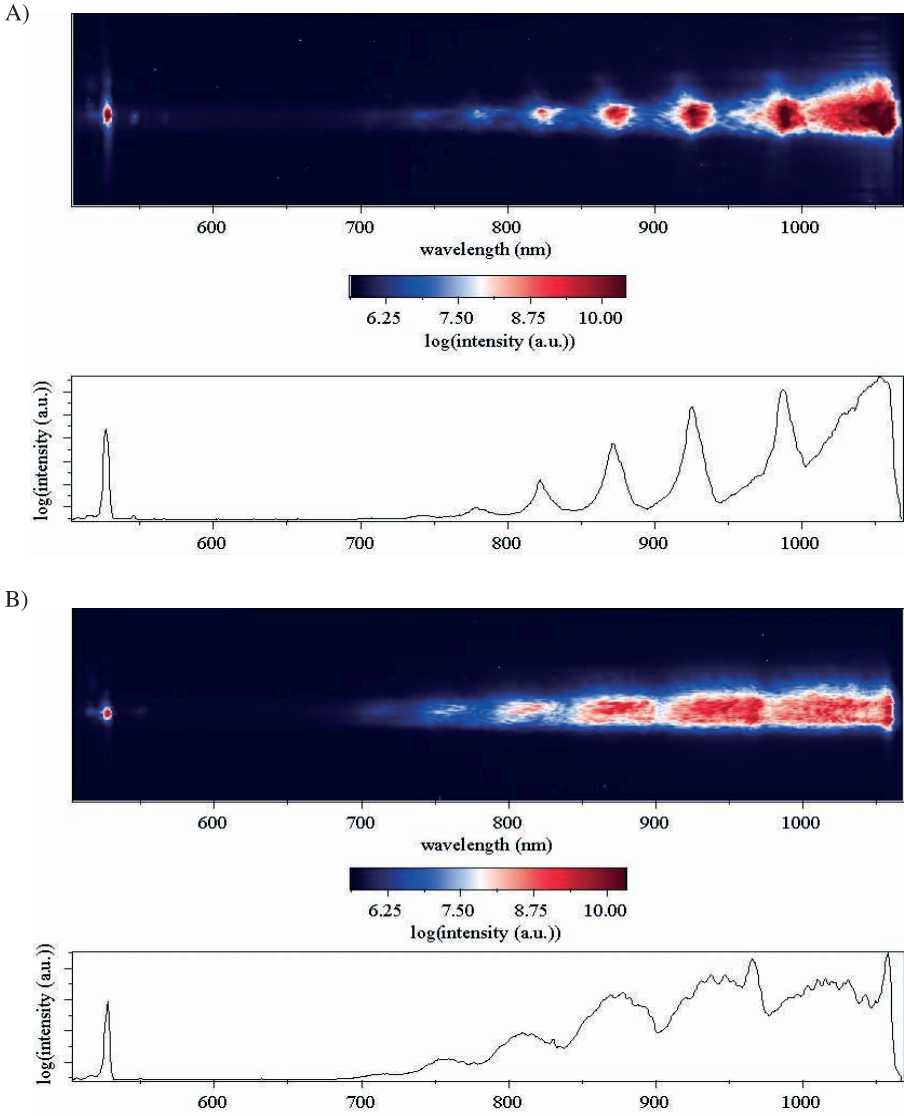


Figure 2. Transmitted beam spectra with (a) $n_e = 4 \times 10^{18} \text{ cm}^{-3}$ and $I = 2 \times 10^{19} \text{ W cm}^{-2}$ and (b) $n_e = 7.5 \times 10^{18} \text{ cm}^{-3}$ and $I = 1 \times 10^{19} \text{ W cm}^{-2}$.

the pulse, resulting in localized pump depletion. This large intensity ramp is then able to drive a large-amplitude plasma wave, which can act as a sufficiently large seed to stimulate the growth of FRS. Once FRS is initiated, the smaller- k_p plasma wave destroys the favourable long-length uniform-density plasma in which the large-angle instabilities thrive, and this together with the plasma heating due to these initial instabilities can effectively damp the large-angle Raman scattering at later times.

The evidence for this behaviour is clearly seen in figure 2(a). This shows the transmitted laser light spectrum for two different densities. Figure 2(a) shows up to eight satellite frequencies of the transmitted light on the blue-shifted side of the

fundamental laser frequency, plotted as the logarithm of intensity. The satellites are very clearly differentiated from one another and are constantly spaced by intervals of the plasma frequency. The spectrum has a similar character on the red side of the fundamental. One can see why the Raman scattering in plasmas is so named owing to the analogy to Raman scattering from molecules.

However, one basic difference exists between plasma Raman scattering and molecular Raman scattering, and that is the excitation of the plasma wave. The plasmons that constitute the plasma wave are not fixed quantum states. As the plasma wave grows to a large amplitude, and in particular when the plasma wave amplitude $\delta n/n_0$ approaches the initial plasma density n_0 , then the plasma wave can no longer be described as the linear superposition of the generated ω_p plasmons. Indeed the high density values tend to form peaks whereas the low density values form shallow troughs. This nonlinearly steepened plasma wave can be Fourier decomposed into its harmonic constituents as follows:

$$\frac{n^m}{n_0} = \frac{m^m}{2^{m-1}m!} \left(\frac{\delta n}{n_0}\right)^m,$$

where n^m is the amplitude of the m th harmonic of the plasma wave of peak amplitude $\delta n/n_0$. One can therefore see why side bands are so efficiently generated even though the growth of the FRS predicts that in 1 ps there is barely enough time for the the first electromagnetic side band to grow to large amplitude. Evidently the cascading is evidence of the scattering from the nonlinear steepened plasma wave, rather than a stepwise scattering of the successive electromagnetic side bands off a linear plasma wave (i.e. one that has a harmonic content only at ω_p).

4. Evidence of wave breaking

Clearly increasing the growth of the plasma wave as a result of further increases in the FRS growth rate cannot lead to an indefinitely increasing plasma wave amplitude. Mori *et al.* [7] have derived the spatiotemporal growth rates for the FRS instability in the relativistic regime ($a_0 > 1$). They found that the FRS growth rate actually saturates with increasing intensity and, in this regime, one can only achieve further plasma wave growth by its dependence on density. This is shown in figure 2(b), where a higher density is used with all other parameters the same as in figure 2(a). The side bands can still be discerned in this figure (with a slightly greater separation owing to the dependence of the plasma frequency on density: $\omega_p = n_0 e^2 / \varepsilon_0 m_e$). However, the side bands are noticeably broader. This occurs although the scattering is over the same pulse length as before. This increased width suggests that the scattering plasma wave is losing coherence.

5. High-energy electron production and the dependence on wave breaking

The exact reason for this loss of coherence is demonstrated by the spectrum of electrons accelerated by the generated plasma wave. This is shown in figure 3. The figure shows that, even at $4 \times 10^{18} \text{ cm}^{-3}$, when the plasma wave is still coherent, there are a significant number of electrons accelerated to quite high energy (up to 13 MeV before they fall below the detection limit of our detector). This is probably due to the high temperature that such plasmas can reach owing to the optical field ionization, and the presence of other large-angle electron plasma oscillations. In

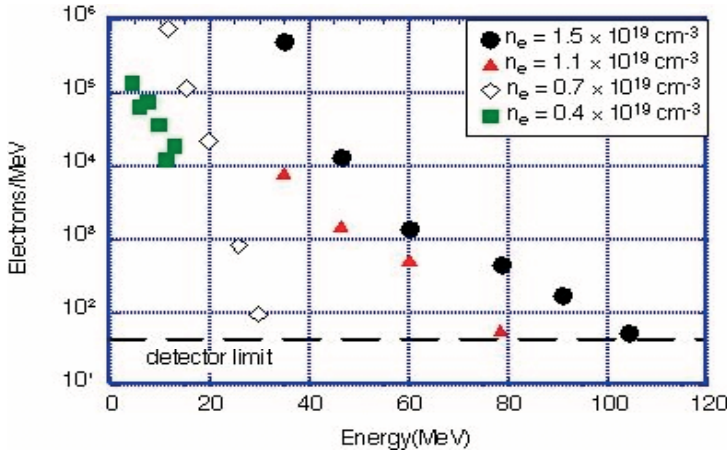


Figure 3. Electron spectra for different densities.

the high electric fields of the plasma wave, it is possible to accelerate these electrons further to high energies, even if they are not trapped for long distances by the plasma wave. However, one can see that, as the density is increased to $7.5 \times 10^{18} \text{ cm}^{-3}$, the number and maximum energy of the electrons increase markedly. This is even more so as the plasma wave growth rate is increased at yet higher densities. One can see that, not only is the maximum energy of the electron distribution increasing, but also it is gaining a significant ‘tail’ to the distribution that can no longer be fitted by a single Maxwellian profile. If one considers all the electrons accelerated, and not just those within the acceptance cone of our detector, one finds 10^{12} relativistic electrons or more, or, in other words, almost all the electrons from within the focal volume over a Rayleigh length. Clearly such a huge fraction of accelerated electrons cannot be simply explained by trapping of hot electrons. The electrons are actually generated by wave breaking [4]. The forces on the electrons forming the peaks of the nonlinear plasma wave are so great that the restoring force that they generate is no longer sufficient to return them to their initial displacement. Indeed charge sheets can cross longitudinally such that, instead of feeling a returning force, some of the electrons (those travelling in the same direction as the phase velocity of the plasma wave) can feel a continuing acceleration in the direction in which they were travelling. Once they can reach relativistic speeds, they can stay in phase with the plasma wave until they gain enough energy that they begin to outrun the wave and so become dephased from it. A simple treatment that considers a sinusoidal plasma wave shows that the maximum energy to which electrons can be accelerated before dephasing is of the order $2\gamma_p^2(\delta n/n_0)m_e c^2$, where γ_p is the phase velocity of the plasma wave, and in the underdense regime it is roughly given by $\gamma_p \approx \omega_0/\omega_p$. So, for densities around 10^{19} cm^{-3} , $\gamma_p \approx 10$, and the maximum expected energy is approximately 100 MeV. Hence, once the wave fully wave breaks, one can see that a significant number of electrons are accelerated until they are dephased from the wave.

Hence the broadening of the satellites in the transmitted spectra is a clear signature of the onset of wave breaking. Indeed, at higher densities, the broad-

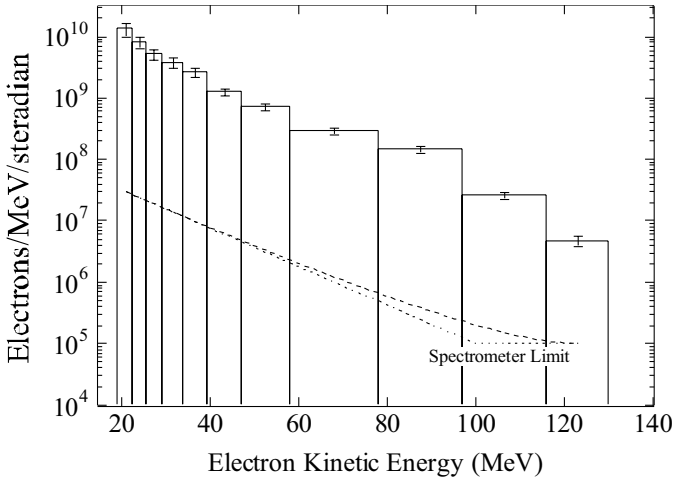


Figure 4. Highest-energy electrons recorded using strip detectors.

ening is so severe that it becomes difficult to distinguish the individual satellites. Note also that there is clear evidence of the increased growth of the FRS at higher densities from figure 2(a) to figure 2(b) even though the intensity of the second shot was slightly lower. This reiterates the weak dependence of the FRS growth rates on intensity in this regime.

6. Highest-energy electron recorded and significance of non-Maxwellian distribution

Figure 4 shows an electron spectrum taken using the strip detectors instead of the individual silicon barrier detectors. The use of the strip array allows one to obtain an energy spectrum of the accelerated electrons at much better resolution and also allows slightly greater collection and thus higher sensitivity. This particular shot was taken at a density of around $2 \times 10^{19} \text{ cm}^{-3}$, for which the maximum expected linear dephased energy is 50 MeV. Clearly some electrons are accelerated beyond this energy. Indeed a few electrons are accelerated to more than twice this energy. It has been suggested by Gordon *et al.* [11] that this acceleration beyond the linear dephasing limit may well be due to the influence of the large current of electrons initially accelerated by the wave breaking. In effect this initial bunch of electrons can set up a large wake in its tail as it travels through the plasma and can accelerate electrons trailing behind to even higher energies, in an almost two-step process.

7. Discussion

It has been shown that an intense laser beam travelling through underdense plasma is highly susceptible to the Raman forward scatter instability. This instability can grow to large amplitude owing to the pulse erosion of the front of the intense pulse. The growth can be sufficient to modulate the laser beam fully and to grow a large-amplitude plasma wave in its wake. Wave breaking of this plasma wave can efficiently produce an intense source of high-energy electrons. The possibility of using these intense electron sources has already been shown for

many applications, such as the generation of short-lived radioisotopes [12], γ -ray radiography [13] and neutron production [14]. As higher-repetition-rate lasers with these intensities become increasingly common, so the prospect of the use of these high-repetition-rate electron sources [15] appears to be bright.

References

- [1] TAJIMAN, T., and DAWSON, J., 1979, *Phys. Rev. Lett.*, **43**, 267.
- [2] DRAKE, J. F., KAW, P. K., LEE, Y. C., SCHMIDT, G., LIU, C. S., and ROSENBLUTH, M. N., 1974, *Phys. Fluids*, **17**, 778.
- [3] FORSLUND, D. W., KINDEL, J. M., and LINDMAN, E. L., 1975, *Phys. Fluids*, **18**, 1002.
- [4] MODENA, A., NAJMUDIN, Z., DANGOR, A. E., CLAYTON, C. E., MARSH, K. A., JOSHI, C., MALKA, V., DARROW, C. B., DANSON, C., NEELY, D., and WALSH, F. A., 1995, *Nature*, **377**, 606.
- [5] MALKA, V., COULAUD, C., GEINDRE, J. P., LOPEZ, V., NAJMUDIN, Z., NEELY, D., and AMIRANOFF, F., 2000, *Rev. scient. Instrum.*, **71**, 2329.
- [6] NAJMUDIN, Z., 1995, PhD Thesis, Imperial College, University of London.
- [7] MORI, W. B., DECKER, C. D., HINKEL, D. E., and KATSIOULEAS, T., 1994, *Phys. Rev. Lett.*, **72**, 1482.
- [8] NAJMUDIN, Z., ALLOTT, R., AMIRANOFF, F., CLARK, E. L., DANSON, C. N., GORDON, D. F., JOSHI, C., KRUSHELNICK, K., MALKA, V., NEELY, D., SALVATI, M. R., SANTALA, M. I. K., TATARAKIS, M., and DANGOR, A. E., 2000, *IEEE Trans. Plasma Sci.*, **28**, 1084.
- [9] DECKER, C. D., MORI, W. B., and KATSIOULEAS, T., 1994, *Phys. Rev. E*, **50**, R3338.
- [10] GORDON, D. F., HAFIZI, B., SPRANGLE, P., HUBBARD, R. F., PENANO, J. R., and MORI, W. B., 2001, *Phys. Rev. E*, **64**, 046 404.
- [11] GORDON, D., TZENG, K. C., CLAYTON, C. E., DANGOR, A. E., MALKA, V., MARSH, K. A., MODENA, A., MORI, W. B., MUGGLI, P., NAJMUDIN, Z., NEELY, D., DANSON, C., and JOSHI, C., 1998, *Phys. Rev. Lett.*, **80**, 2133.
- [12] SANTALA, M. I. K., NAJMUDIN, Z., CLARK, E. L., TATARAKIS, M., KRUSHELNICK, K., DANGOR, A. E., MALKA, V., FAURE, J., ALLOT, R., and CLARKE, R. J., 2001, *Phys. Rev. Lett.*, **86**, 1227.
- [13] EDWARDS, R. D., SINCLAIR, M. A., GOLDSACK, T. J., KRUSHELNICK, K., BEG, F. N., CLARK, E. L., DANGOR, A. E., NAJMUDIN, Z., TATARAKIS, M., WALTON, B., ZEPF, M., LEDINGHAM, K. W. D., SPENCER, I., NORREYS, P. A., and CLARKE, R. J., 2002, *Appl. Phys. Lett.* **80**, 2129.
- [14] LEEMANS, W. P., RODGERS, D., CATRAVAS, P. E., GEDDES, C. G. R., FUBIANI, G., ESAREY, E., SHADWICK, B. A., DONAHUE, R., and SMITH, A., 2001, *Phys. Plasmas*, **8**, 2510.
- [15] MALKA, V., FAURE, J., MARQUES, J. R., AMIRANOFF, F., ROUSSEAU, J. P., RANC, S., CHAMBERET, J. P., NAJMUDIN, Z., WALTON, B., MORA, P., and SOLODOV, A., 2001, *Phys. Plasmas*, **8**, 2605.